Two-dimensional electronic spectra from the hierarchical equations of motion method: Application to model dimers

Liping Chen,[1] Renhui Zheng,[1] Qiang Shi,[1,a)] and YiJing Yan[2]
[1]*Beijing National Laboratory for Molecular Sciences, State Key Laboratory for Structural Chemistry of Unstable and Stable Species, Institute of Chemistry, Chinese Academy of Sciences, Zhongguancun, Beijing 100190, China*
[2]*Department of Chemistry, Hong Kong University of Science and Technology, Kowloon, Hong Kong SAR, China*

(Received 30 November 2009; accepted 23 December 2009; published online 14 January 2010)

We extend our previous study of absorption line shapes of molecular aggregates using the Liouville space hierarchical equations of motion (HEOM) method [L. P. Chen, R. H. Zheng, Q. Shi, and Y. J. Yan, J. Chem. Phys. **131**, 094502 (2009)] to calculate third order optical response functions and two-dimensional electronic spectra of model dimers. As in our previous work, we have focused on the applicability of several approximate methods related to the HEOM method. We show that while the second order perturbative quantum master equations are generally inaccurate in describing the peak shapes and solvation dynamics, they can give reasonable peak amplitude evolution even in the intermediate coupling regime. The stochastic Liouville equation results in good peak shapes, but does not properly describe the excited state dynamics due to the lack of detailed balance. A modified version of the high temperature approximation to the HEOM gives the best agreement with the exact result. © *2010 American Institute of Physics*. [doi:10.1063/1.3293039]

I. INTRODUCTION

The multidimensional optical spectroscopy has developed into a powerful tool to investigate structure and dynamics of complex molecular systems over the last decade.[1–5] Although the initial efforts have focused on the two-dimensional infrared (2D IR) spectroscopy,[5–7] recent experiments have extended to studies of electronic structure and dynamics in the optical regime.[8–15] Recently, the 2D electronic spectroscopy has been applied to various types of molecular aggregates, such as *J*-aggregates[16] and light harvesting complex in photosynthetic systems,[17,18] where important information on structure and electronic interaction, excited state dynamics, and electronic energy transfer (EET) processes have been obtained.[10–13,19–21] In particular, oscillations in the peaks of the 2D electronic spectra have revealed that quantum coherence plays an important role in excitation energy transfer in various systems such as the light harvesting complexes[11,12] and conjugated polymer.[14,15]

Theory and simulation play an important role in explaining the experimental 2D spectra and extracting important structural and dynamical information.[2,3,5,20,22] A particular challenge in calculating the nonlinear optical spectra of molecular aggregates is that both the intermolecular electronic coupling and electron-phonon coupling play an important role in the excitonic dynamics in these systems. Traditional perturbation theory based on either the Fermi's golden rule or the second order quantum master equations (QMEs) becomes invalid when these interactions are of comparable magnitude (i.e., in the intermediate coupling regime).

In literature, different methods have been developed to calculate the third order optical response and 2D spectra of molecular aggregates. In the modified Redfield equation approach originally developed by Mukamel and co-workers,[2,9,23–25] the diagonal energy fluctuations are treated nonperturbatively, while the off-diagonal system-bath couplings are treated via second order perturbation. More recently, population transfer and coherence transfer were incorporated in the modified Redfield equation method.[26,27] Methods that calculate the molecular polarization based on a nonperturbative treatment of the field-matter interaction were also employed by several groups in calculating the photon echo (PE) signal and 2D spectra.[28–33] However, in these methods, the electron-phonon interaction is treated perturbatively using the Redfield theory, or the time-nonlocal (TNL) QME methods, which may not be valid when the electron-phonon interaction is comparable or larger than the intermolecular coupling or temperature.

Another often employed strategy to study nonlinear optical response is based on a semiclassical treatment of the nuclear degrees of freedom (DOFs),[22] which can be traced back to the Kubo-Anderson line shape theory.[34,35] In this approach, the energy gaps and electronic couplings fluctuate as the nuclear degrees of freedom evolve on the ground electronic state, while the back reaction of the electronic DOFs to the nuclear DOFs is neglected. Such treatment of the electron-phonon coupling has lead to the numerical integration of the Schrödinger equation (NISE) to calculate the 2D IR spectra,[36–38] and the stochastic Liouville equation (SLE) method when assuming exponential correlation for the energy gap fluctuations.[39,40] The NISE/SLE methods can describe the effect of solvent dynamics on the 2D spectra, which is often not available in the methods where the electron-phonon coupling are treated pertubatively. However,

a)Electronic mail: qshi@iccas.ac.cn.

since the solvent dynamics is described solely on the ground electronic state, the NISE/SLE methods may not able to capture the excited state dynamics that is important to explain the 2D spectra signals.[41–43] In addition, neglecting the back reaction of the electronic DOFs to the nuclear DOFs is well known to cause problems with detailed balance,[44] which may also lead to errors in calculating the excited state dynamics and the 2D spectra.

In a previous paper,[45] we applied the recently developed hierarchical equations of motion (HEOM) formalism[46–51] to calculate the absorption line shapes of molecular aggregates based on the dipole-dipole correlation function, and found that the TNL QME is generally not valid in calculating the linear optical response and the absorption spectra. Also, Tanimura and co-workers[48,52–54] have applied the HEOM method to calculate 2D IR spectra, Ishizaki and Fleming[55,56] have applied a high temperature version of the HEOM to investigate the coherent and incoherent EET dynamics in a model dimer and the Fenna–Matthews–Olson (FMO) complex,[57] and pointed out the inadequacy of traditional Redfield theory and Förster theory in describing EET processes.

In this paper, by extending our previous study of the absorption line shapes, we apply the HEOM method to calculate the third order optical response function and 2D spectra in model dimer systems, and assess the applicability of the approximate methods of pertubative QMEs, SLE, and high temperature approximations to the HEOM. The remaining sections of this paper are arranged as follows. In Sec. II, we present the HEOM and related theories. In Sec. III, we apply the HEOM method to calculate third order optical response functions and 2D spectra for a model dimer system, and compare them to the results of approximate methods. Conclusions and discussions are made in Sec. IV.

II. THEORY

A. Model Hamiltonian

We consider a molecular system that couples to the electronic-magnetic field, the total Hamiltonian can be written as

$$H(t) = H_{\mathrm{mol}} - \boldsymbol{\mu}\cdot\mathbf{E}(t), \tag{1}$$

where H_{mol} is the Hamiltonian of the molecular aggregate, $\mathbf{E}(t)$ is the classical electromagnetic field, and $\boldsymbol{\mu}$ is the dipole operator. The equations below are formulated for a Frenkel exciton model of N two-level molecules coupled to a phonon bath. The total dipole operator $\boldsymbol{\mu}$ is defined as

$$\boldsymbol{\mu} = \sum_{m=1}^{N} \boldsymbol{\mu}_m (a_m + a_m^+), \tag{2}$$

with a_m^+ and a_m being the creation and annihilation operators of the electronic excitation on the mth molecule. The molecular Hamiltonian H_{mol} is written as

$$H_{\mathrm{mol}} = H_e + H_{\mathrm{ph}} + H_{e\text{-ph}}. \tag{3}$$

Here, H_e describes the electronic DOF,

$$H_e = \sum_{m=1}^{N} \epsilon_m a_m^+ a_m + \sum_{m=1}^{N}\sum_{n<m} J_{nm}(a_m^+ a_n + a_n^+ a_m), \tag{4}$$

where ϵ_m is the on-site transition energy and J_{nm} is the intermolecular coupling. H_{ph} describes the nuclear (phonon) DOFs. It is assumed that the electronic excitation on the mth molecule couples independently to its own harmonic bath, such that

$$H_{\mathrm{ph}} = \sum_{m=1}^{N}\sum_{j=1}^{N_b^m}\left(\frac{p_{mj}^2}{2} + \frac{1}{2}\omega_{mj}x_{mj}^2\right), \tag{5}$$

where N_b^m is the number of bath modes coupled to molecule m, x_{mj} and p_{mj} are the mass weighted position and momentum of the jth harmonic oscillator bath mode with frequency ω_{mj}. For simplicity, we set $\hbar = 1$ throughout this paper.

The electron-phonon coupling $H_{e\text{-ph}}$ is assumed to cause only electronic energy fluctuations that are independent for each chromophore. $H_{e\text{-ph}}$ is also assumed to be linear in the bath coordinates, such that

$$H_{e\text{-ph}} = \sum_{m=1}^{N}\sum_{j=1}^{N_b^m} c_{mj}x_{mj}a_m^+ a_m = \sum_{m=1}^{N} F_m a_m^+ a_m \tag{6}$$

where the collective bath coordinate F_m is defined as $F_m = \sum_{j=1}^{N_b^m} c_{mj}x_{mj}$.

The spectral density $J_m(\omega)$ is defined as

$$J_m(\omega) = \frac{\pi}{2}\sum_{j=1}^{N_b^m}\frac{c_{mj}^2}{\omega_{mj}}\delta(\omega-\omega_{mj}). \tag{7}$$

The correlation function of the collective bath coordinate F_m is then given by

$$C_m(t) = \frac{1}{Z_B}\mathrm{Tr}(e^{-\beta H_{\mathrm{ph}}}e^{iH_{\mathrm{ph}}t}F_m e^{-iH_{\mathrm{ph}}t}F_m) = \frac{1}{\pi}\int_{-\infty}^{\infty} d\omega \frac{e^{-i\omega t}J(\omega)}{1-e^{-\beta\omega}}. \tag{8}$$

B. Third order optical response functions

When the electromagnetic field is weak, various observables in linear and nonlinear optical spectroscopy can be obtained by applying perturbation theory to the field-matter interaction, and expressed into optical response functions in terms of dipole correlation functions.[22] The following derivation is similar to those in many previous papers,[5,22,52,53,58] and it is given below mainly for the reason of completeness.

The 2D spectra probe the third order optical response, where the electronic polarization $\mathbf{P}$ can be obtained as

$$\mathbf{P}^{(3)}(t) = i^3 N\int_0^{\infty} dt_3\int_0^{\infty} dt_2\int_0^{\infty} dt_1 R^{(3)}(t_3,t_2,t_1) \mathbf{E}(\mathbf{r},t-t_3)\mathbf{E}(\mathbf{r},t-t_3-t_2)\mathbf{E}(\mathbf{r},t-t_3-t_2-t_1). \tag{9}$$

Here, N is the number density of the molecule, $R^{(3)}$ is the third order optical response function, which, by neglecting its rotational dependence, can be written as:

$$R^{(3)}(t_3,t_2,t_1) = \langle[[[\mu(t_3+t_2+t_1),\mu(t_2+t_1)],\mu(t_1)],\mu(0)]\rho_0\rangle$$
$$= \langle\mu\mathcal{G}(t_3)\mathcal{V}\mathcal{G}(t_2)\mathcal{V}\mathcal{G}(t_1)\mathcal{V}\rho_0\rangle, \quad (10)$$

where ρ_0 is the equilibrium system operator, $\mu(t) = e^{iH_{\rm mol}t}\mu e^{-iH_{\rm mol}t}$. The Liouville space superoperators $\mathcal{V}$ and $\mathcal{G}(t)$ are defined as $\mathcal{V}\rho=[\mu,\rho]$, $\mathcal{G}(t)\rho=e^{-iH_{\rm mol}t}\rho e^{iH_{\rm mol}t}$, respectively.

In three pulse PE (3PE) and 2D spectra experiments, three laser pulses with wave-vectors $\mathbf{k}_1$, $\mathbf{k}_2$, and $\mathbf{k}_3$ are sent through the sample, and the third order nonlinear response signal is detected along a phase-matched direction $\mathbf{k}_S$.[3,5,36,37,58] By applying the rotating wave approximation, the total response function for the 3PE signal can be obtained from the rephasing ($\mathbf{k}_{\rm I}=-\mathbf{k}_1+\mathbf{k}_2+\mathbf{k}_3$) and nonrephasing ($\mathbf{k}_{\rm II}=\mathbf{k}_1-\mathbf{k}_2+\mathbf{k}_3$) contributions: $R^{(3)}(t_3,t_2,t_1)=R_{rp}(t_3,t_2,t_1)+R_{nr}(t_3,t_2,t_1)$, where they can be conveniently calculated using the following equations,[26,59]

$$R_{rp}(t_3,t_2,t_1) = \langle\mu_-\mathcal{G}(t_3)\mathcal{V}_+\mathcal{G}(t_2)\mathcal{V}_+\mathcal{G}(t_1)\mathcal{V}_-\rho_0\rangle, \quad (11)$$

$$R_{nr}(t_3,t_2,t_1) = \langle\mu_-\mathcal{G}(t_3)\mathcal{V}_+\mathcal{G}(t_2)\mathcal{V}_-\mathcal{G}(t_1)\mathcal{V}_+\rho_0\rangle, \quad (12)$$

where $\mathcal{V}_\pm\rho=[\mu_\pm,\rho]$, $\mu_-=\Sigma_{m=1}^N\mu_m a_m$, and $\mu_+=\Sigma_{m=1}^N\mu_m a_m^+$.

Expanding the commutators leads to the following forms of R_{rp} and R_{nr}

$$R_{rp}(t_3,t_2,t_1) = \Phi_1(t_3,t_2,t_1) + \Phi_2(t_3,t_2,t_1) - \Phi_3(t_3,t_2,t_1), \quad (13)$$

$$R_{nr}(t_3,t_2,t_1) = \Phi_4(t_3,t_2,t_1) + \Phi_5(t_3,t_2,t_1) - \Phi_6(t_3,t_2,t_1), \quad (14)$$

where the individual response functions $\Phi_1-\Phi_6$ are defined as

$$\Phi_1(t_3,t_2,t_1) = \langle\mu_-\mathcal{G}(t_3)\{\mathcal{G}(t_2)[\mu_+\mathcal{G}(t_1)(\rho_0\mu_-)]\mu_+\}\rangle,$$
$$\Phi_2(t_3,t_2,t_1) = \langle\mu_-\mathcal{G}(t_3)\{\mu_+\mathcal{G}(t_2)[\mathcal{G}(t_1)(\rho_0\mu_-)\mu_+]\}\rangle,$$
$$\Phi_3(t_3,t_2,t_1) = \langle\mu_-\mathcal{G}(t_3)\{\mu_+\mathcal{G}(t_2)[\mu_+\mathcal{G}(t_1)(\rho_0\mu_-)]\}\rangle,$$
$$\Phi_4(t_3,t_2,t_1) = \langle\mu_-\mathcal{G}(t_3)\{\mathcal{G}(t_2)[\mathcal{G}(t_1)(\mu_+\rho_0)\mu_-]\mu_+\}\rangle, \quad (15)$$
$$\Phi_5(t_3,t_2,t_1) = \langle\mu_-\mathcal{G}(t_3)\{\mu_+\mathcal{G}(t_2)[\mu_-\mathcal{G}(t_1)(\mu_+\rho_0)]\}\rangle,$$
$$\Phi_6(t_3,t_2,t_1) = \langle\mu_-\mathcal{G}(t_3)\{\mu_+\mathcal{G}(t_2)[\mathcal{G}(t_1)(\mu_+\rho_0)\mu_-]\}\rangle.$$

The above terms $\Phi_1-\Phi_6$ correspond to different Liouville space pathways described by the double-sided Feynman diagrams in Fig. 1. Their contributions to the third order optical response can be classified as ground state bleaching (GSB), excited stimulated emission (ESE), and excited state absorption (ESA).[22] The relation between the individual terms $\Phi_1-\Phi_6$ and the four third order nonlinear response functions R_1-R_4 (Ref. 22) are also given in Fig. 1. In the impulsive limit, the (absorptive part of the) 2D spectra are

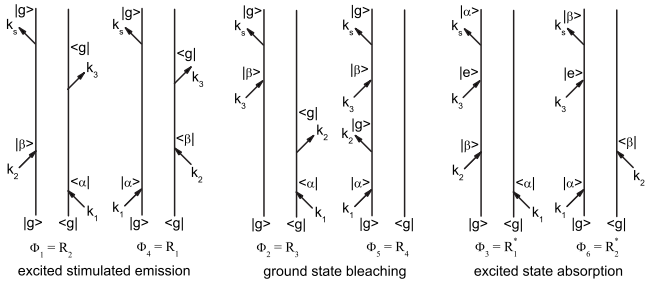

FIG. 1. Double-sided Feynman diagrams for the rephasing and nonrephasing signals. They can be classified into GSB, ESE, and ESA contributions. $|g\rangle$ is the ground state, $|\alpha\rangle$ and $|\beta\rangle$ are the one-exciton states, and $|e\rangle$ is the two-exciton state.

calculated as the real part of the following sum of the double Fourier–Laplace transforms of $R_{nr}(t_3,t_2,t_1)$ and $R_{rp}(t_3,t_2,t_1)$ with respect to t_1 and t_3:[2,5,37,58]

$$S(\omega_3,t_2,\omega_1) \equiv \mathrm{Re}\int_0^\infty dt_1\int_0^\infty dt_3[e^{i(\omega_1 t_1+\omega_3 t_3)}R_{nr}(t_3,t_2,t_1) + e^{i(-\omega_1 t_1+\omega_3 t_3)}R_{rp}(t_3,t_2,t_1)]. \quad (16)$$

C. The HEOM and the approximate methods

In this study, the coupling phonon bath spectral density $J_m(\omega)$ of Eq. (7) is assumed to be the same for all molecules, and the Debye type spectral density is used,

$$J(\omega) = \frac{\eta\gamma\omega}{\omega^2+\gamma^2}, \quad (17)$$

which assumes the overdamped Brownian motion for the energy gap fluctuations in the classical (high temperature) limit. The resulting bath correlation function $C_m(t)$ in Eq. (8) can be written into a sum of exponential decaying function in time:

$$C_m(t>0) = \sum_{k=0}^{\infty} c_k e^{-\gamma_k t}, \quad (18)$$

with $\gamma_0=\gamma$ and $\gamma_k=2k\pi/\beta$ $(k\geq 1)$ are the Matsubara frequencies,

$$c_0 = \frac{\eta\gamma}{2}[\cot(\beta\gamma/2) - i], \quad (19)$$

and

$$c_k = \frac{4k\pi\eta\gamma}{(2k\pi)^2-(\beta\gamma)^2}, \quad k\geq 1. \quad (20)$$

The HEOM method is a nonperturbative theory to calculate the reduced system dynamics. We assume that the initial state is equilibrated on the ground electronic state $|g\rangle$, such that $\rho_0=|g\rangle\langle g|\otimes e^{-\beta H_B}/\mathrm{Tr}\,e^{-\beta H_B}$. The formally exact HEOM equation is given by:[46–51]

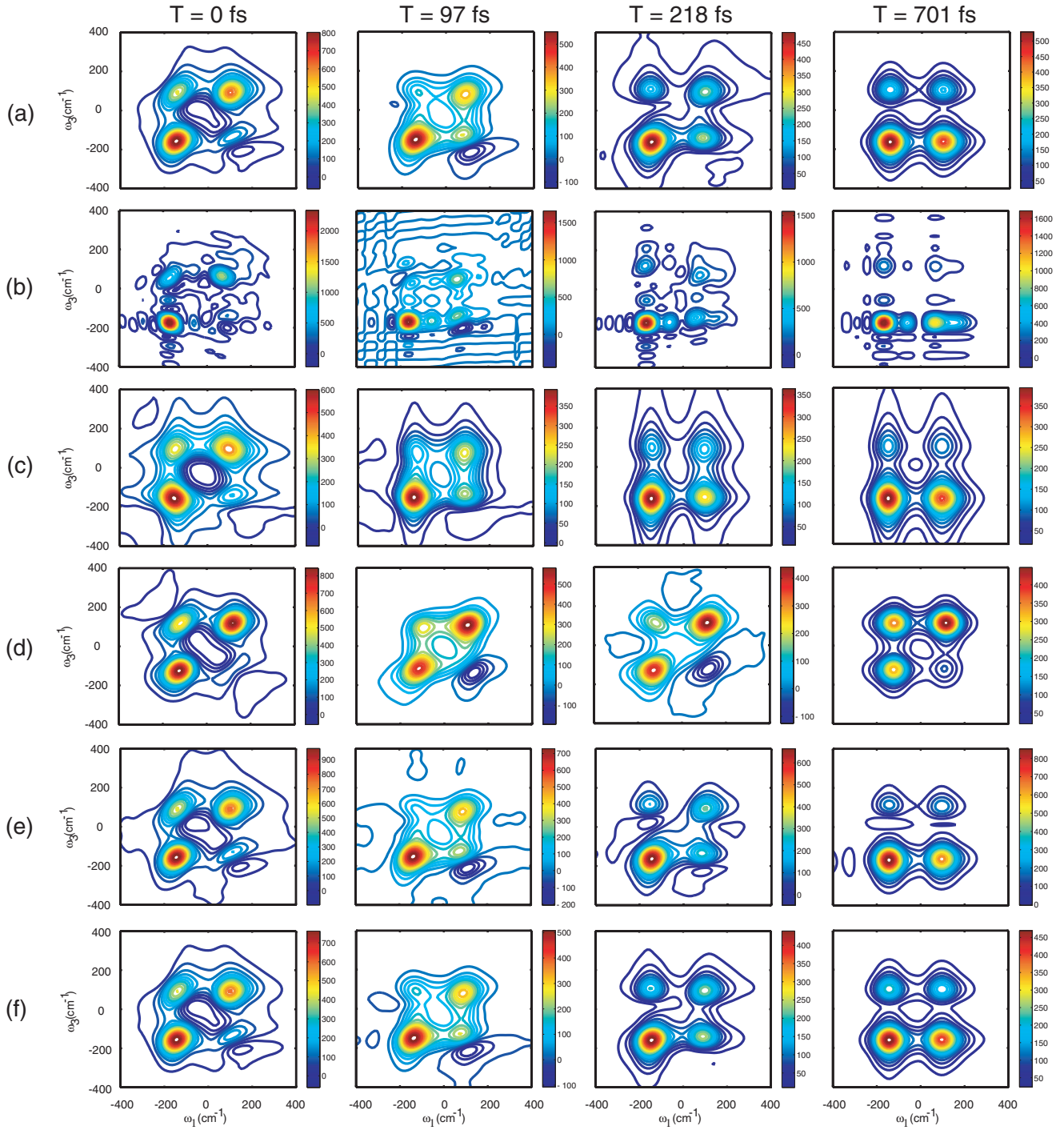

FIG. 2. 2D electronic spectra calculated using different methods (a) HEOM, (b) TNL2, (c) TL2, (d) SLE, (e) HTA, and (f) modified HTA.

$$\frac{d}{dt}\rho_{\mathbf{n}} = -\left(i\mathcal{L} + \sum_{m=1}^{N}\sum_{k} n_{mk}\gamma_k\right)\rho_{\mathbf{n}} - i\sum_{m=1}^{N}\left[a_m^+ a_m, \sum_k \rho_{\mathbf{n}_{mk}^+}\right] - i\sum_{m=1}^{N}\sum_{k} n_{mk}(c_k a_m^+ a_m \rho_{\mathbf{n}_{mk}^-} - c_k^* \rho_{\mathbf{n}_{mk}^-} a_m^+ a_m), \quad (21)$$

where $\mathcal{L}\rho=[H_e,\rho]$. The subscript $\mathbf{n}$ denotes the set of index $\mathbf{n}\equiv\{\mathbf{n}_1,\mathbf{n}_2,\cdots,\mathbf{n}_N\}=\{\{n_{10},n_{11},\cdots\},\cdots,\{n_{N0},n_{N1},\cdots\}\}$, and $\mathbf{n}_{mk}^{\pm}$ differs from $\mathbf{n}$ only by changing the specified n_{mk} to $n_{mk}\pm 1$. The ρ_0 with $\mathbf{0}=\{\{0,0,\cdots\},\cdots,\{0,0,\cdots\}\}$ is the system reduced density operator (RDO) while the other $\rho_{\mathbf{n}}$s are the auxiliary density operators (ADOs). The ADOs contain important information about the system-bath correlations, which are essential in capturing the nonequilibrium solvent dynamics.[45,46,56]

As μ does not depend on the bath DOFs, the ensemble average in Eqs. (15) can be performed first by tracing over the bath DOFs. For example,

$$\Phi_1(t_3,t_2,t_1) = \mathrm{Tr}_S[\mathrm{Tr}_B(\mu_-\mathcal{G}(t_3)\{\mathcal{G}(t_2)[\mu_+\mathcal{G}(t_1)\times(\rho_0\mu_-)]\mu_+\})], \quad (22)$$

which can be calculated by doing the propagation of the system reduced operator with $\rho_S(0)=(|g\rangle\langle g|\mu_-)$ and multi-

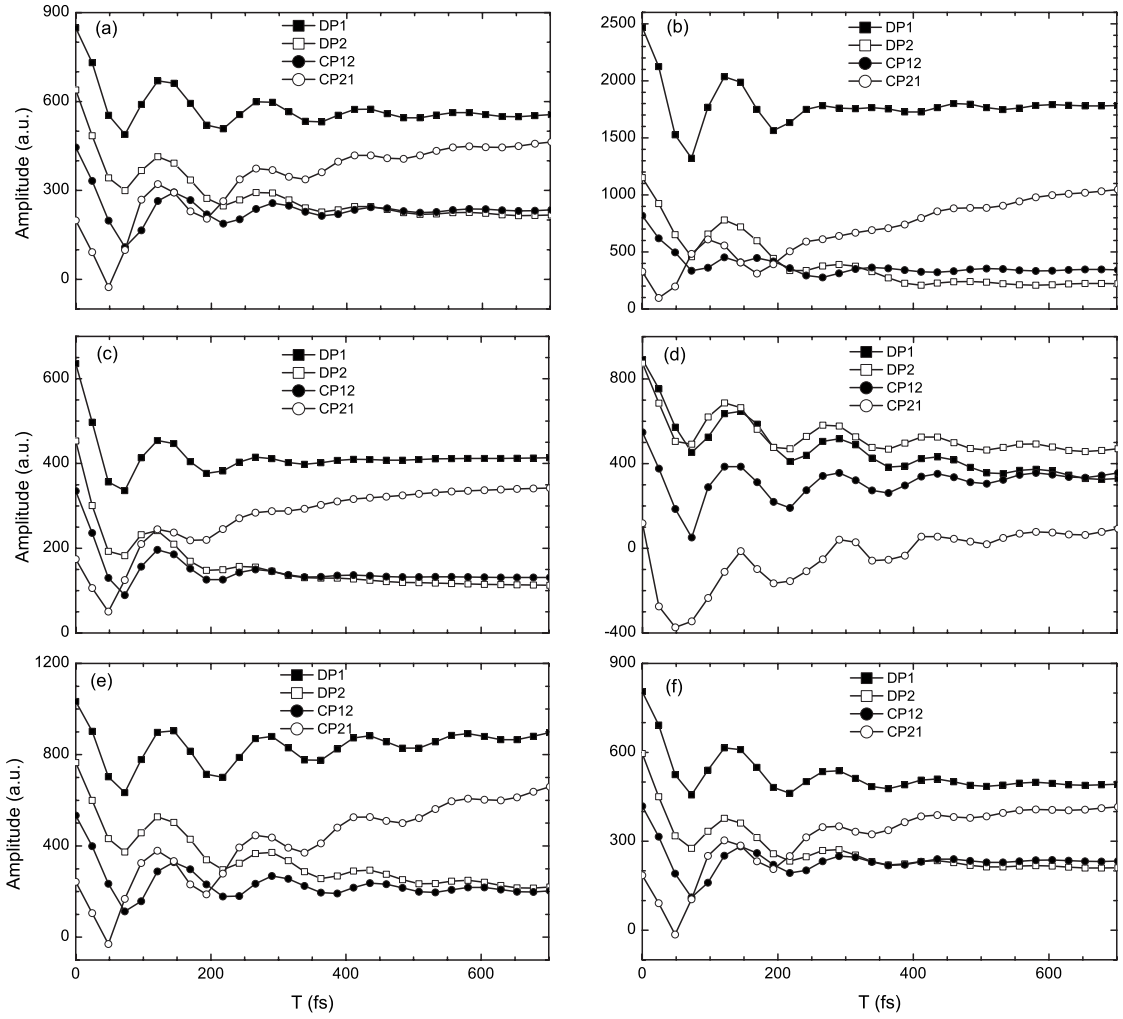

FIG. 3. Oscillations of the amplitudes of the four major peaks in the 2D electronic spectra calculated using different methods (a) HEOM, (b) TNL2, (c) TL2, (d) SLE, (e) HTA, and (f) modified HTA.

plying the dipole operators to the RDO and ADOs at time t_1, t_2, and t_3.[48,52,53] Computation of the reduced dynamics using Eq. (21) is essentially the same as in our previous paper,[45] using the numerical algorithms developed in Refs. 49 and 60. The matrix form of the exciton Hamiltonian and the dipole operator can be found in Ref. 9.

In this study, several approximate methods related to the HEOM are also investigated. These include the perturbative TNL and time-local (TL) QME, the SLE, and high-temperature approximation (HTA) to HEOM. Detailed formulations of these approximate methods can be found in our previous paper.[45] In this study, we also propose a modified version of the HTA, which is obtained by applying the Ishizaki-Tanimura truncating scheme for all the Matsubara frequencies.[48,49] The resulted equation is

$$\frac{d}{dt}\rho_{\mathbf{n}} = -\left(i\mathcal{L} + \gamma\sum_{m=1}^{N} n_m\right)\rho_{\mathbf{n}} - \sum_{m=1}^{N}\left(\frac{\eta}{\beta\gamma} - \frac{\eta}{2}\cot(\beta\gamma/2)\right) \times [a_m^+ a_m,[a_m^+ a_m,\rho_{\mathbf{n}}]] - i\sum_{m=1}^{N}[a_m^+ a_m,\rho_{\mathbf{n}_m^+}] - i\sum_{m=1}^{N} n_m(c_0 a_m^+ a_m \rho_{\mathbf{n}_m^-} - c_0^* \rho_{\mathbf{n}_m^-} a_m^+ a_m). \quad (23)$$

Comparing to the original HTA [Eq. (17) in Ref. 45], the modified HTA in Eq. (23) reduces the effective bath fluctuation from η/β to $\eta\gamma/2\cot(\beta\gamma/2)$, and includes an extra dephasing term as described by the second term in the right-hand side of Eq. (23). In the classical limit $\beta\to 0$, Eq. (23) reduces to the original HTA. We will see later that the modified HTA can give better results at low temperatures.

In the remaining parts of this subsection, we briefly discuss the approximations involved in these methods, as well as their possible limitations. The TNL and TL QMEs are derived under the assumption of weak system-bath coupling, and can be formulated as approximate truncation schemes to the exact HEOM equation.[45,50,61] Recently, the Redfield equation based on similar approximation was found to be invalid in calculating EET dynamics with large reorganization energies.[55,56] We also found that the perturbative TNL QMEs are generally inaccurate in calculating the absorption spectra of molecular aggregates.[45] The SLE is also closely related to the HEOM method: when the nuclear DOFs are treated classically, the SLE can be obtained by applying the high temperature approximate to the HEOM and neglecting the imaginary parts of the bath correlation functions.[45,53] As the imaginary parts of the bath correlation functions are related to the Lamb shift,[62] the SLE is expected to cause fre-

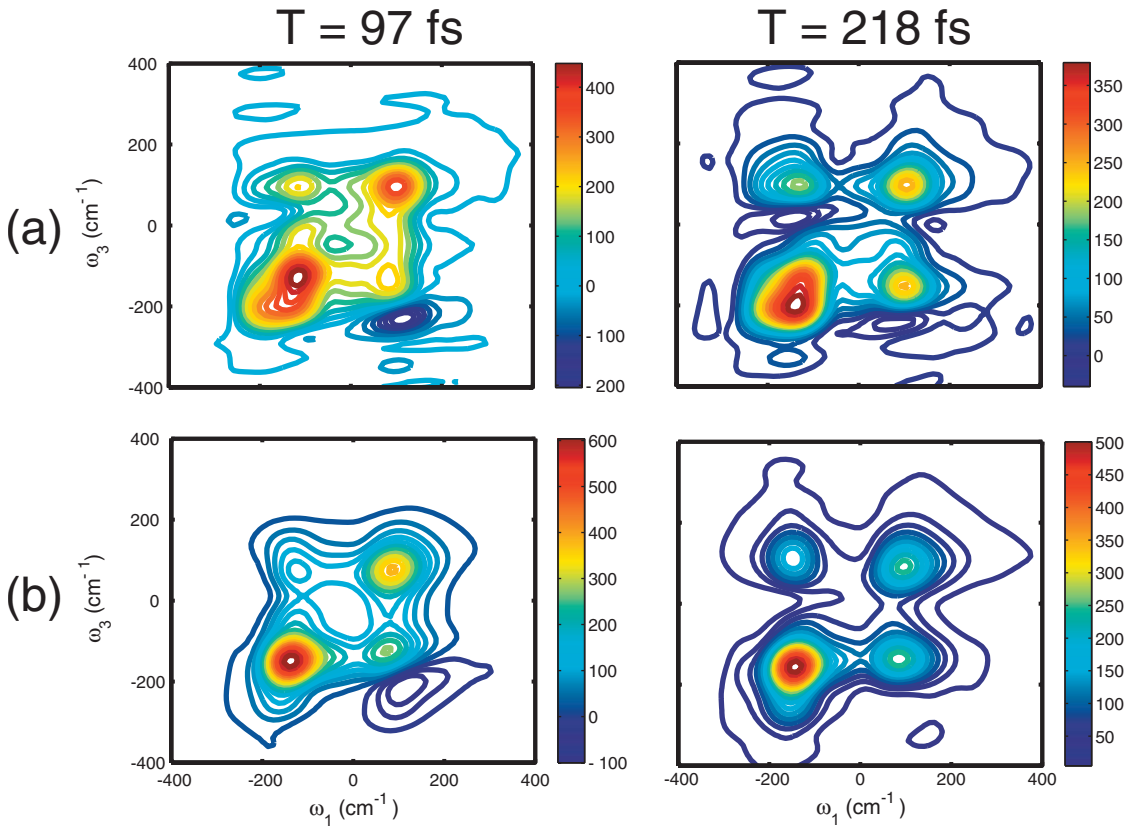

FIG. 4. 2D electronic spectra calculated using higher order perturbative TNL QMEs at $T=97$ and 218 fs. (a) Fourth order and (b) sixth order.

quency shifts in both the linear and nonlinear spectra. Moreover, discarding the imaginary parts of the bath correlation functions also neglects the back reaction of the system to the bath and may cause problems with detailed balance, which could also be problematic in describing excited state dynamics in molecular aggregates. On the other hand, the HTA and modified HTA methods, which include the imaginary part of the bath correlation function, should be able to perform better than the SLE.

III. RESULTS

A. Test case without static disorder

We now apply the HEOM and approximate methods to calculate the 2D spectra $S(\omega_3, t_2=T, \omega_1)$ of a model dimer system. We first investigate the case without static disorder, as this will be a more stringent test to reveal the limits of different approximate methods. Later, we will consider the effect of static disorder and orientation disorder. The parameters used in the simulation are $\epsilon_1=-50$ cm^{-1}, $\epsilon_2=50$ cm^{-1}, $J_{12}=100$ cm^{-1}, $\gamma^{-1}=100$ fs, and $\eta=120$ cm^{-1} corresponding to a reorganization energy of 60 cm^{-1}. In the exciton representation, the eigenvalues of the dimer system are $E_1=-111.8$ cm^{-1} and $E_2=111.8$ cm^{-1}, respectively. The temperature is 77 K in all the calculations.

Figure 2 shows the 2D electronic spectra from different methods. We have used the dipole moments $\mu_1=1$ and $\mu_2=-0.2$ for the two monomers. As in the previous case for absorption spectra, the second order TNL QME gives too narrow peaks and several small spurious peaks when $T\neq 0$ [Fig. 2(b)], which differ drastically from the exact result [Fig. 2(a)]. For the second order TL QME [Fig. 2(c)], the peak widths are similar to the exact result. However, an important difference is that the TL2 spectra miss the correct evolution of the peak shapes: (1) at $T=0$ in the HEOM spectra, the two diagonal peaks (denoted as DP1 at the position $\omega_{1,3}\approx E_1$, and DP2 at $\omega_{1,3}\approx E_2$) are elongated along the diagonal direction, while in the TL2 spectra, they both have a slightly larger antidiagonal width; (2) at longer T, the HEOM spectra evolves to a more symmetric shape, but the TL2 spectra does not capture the correct evolution of the peak shapes. The above shortcoming of the TL2 method is due to the fact that the electron-phonon correlation is not explicitly considered. Similar result has been observed previously in the 2D spectra of a monomer.[59]

The SLE spectra [Fig. 2(d)] agree well with the HEOM result at time $T=0$, except for the small difference for the amplitude of the CP21 cross peak (defined as the main cross peak at $\omega_1\approx E_2$, and $\omega_3\approx E_1$). The shape evolution of the 2D spectra is also observed in the SLE spectra. However, the peak amplitudes in the SLE 2D spectra start to deviate from the exact result at longer times. Eventually, the equilibrated peak intensities differ significantly from those in the exact result. This indicates that the detailed balance problem is rather severe in calculating the 2D spectra of molecular aggregates. As expected, the HTA spectra [Fig. 2(e)] agree much better with the exact result. The modified HTA spectra [Fig. 2(f)] are essentially the same as the HEOM results. We note that the modified HTA is about an order of magnitude faster than the HEOM (the numerically converged HEOM

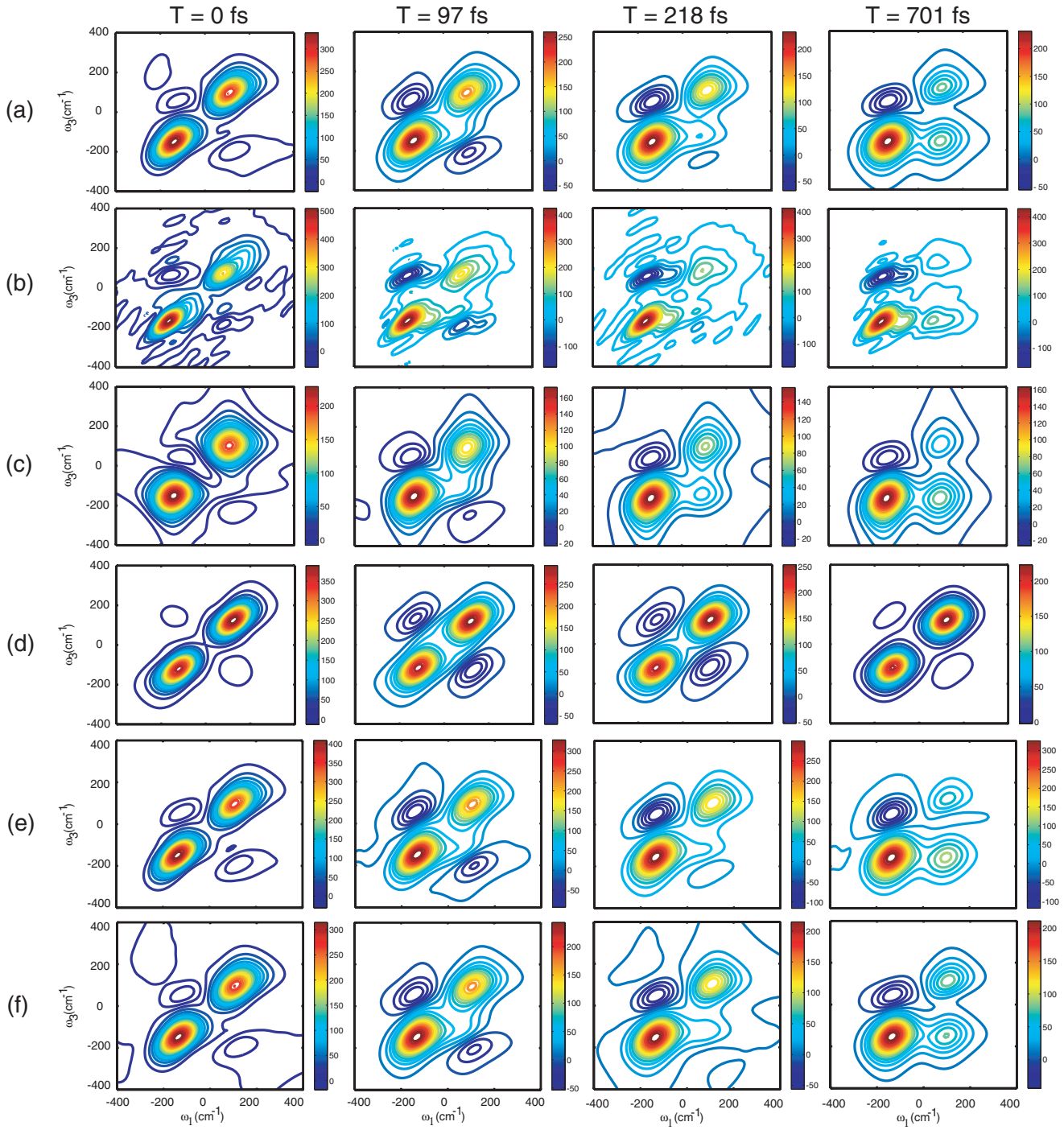

FIG. 5. 2D electronic spectra calculated using different methods in the presence of static disorder. (a) HEOM, (b) TNL2, (c) TL2, (d) SLE, (e) HTA, and (f) modified HTA.

results were obtained by including $K=3$ Matsubara frequencies). Our result shows that the modified HTA has a larger range of applicability than the original HTA, and can be applied to low temperatures and give reasonable results. Similar but different approximate HTA schemes have also been derived in recent literature.[57,63]

The parameters used in our simulation are in the intermediate coupling regime where the intermolecular coupling is comparable to the electron-phonon coupling. In such cases, EET may occur through coherent wavelike motion.[31,33,56,57,64] The experimentally observed oscillation of diagonal and off-diagonal peaks in the 2D spectra is an important indication for such coherent dynamics.[12,14] Oscillations of diagonal and off-diagonal peaks are also observed in the calculated 2D spectra. Figure 3 shows the amplitude evolution of the four main peaks DP1, DP2, CP12, and CP21 calculated using different methods. The TNL2 and TL2 results show the correct behavior although they also show slightly less oscillation than the exact result. On the other hand, the SLE result shows stronger oscillations, and the peaks amplitudes evolute to wrong equilibrated values at long times. The HTA and modified HTA results are essentially the same as the HEOM result.

We also notice the HEOM truncated directly at nth tier,

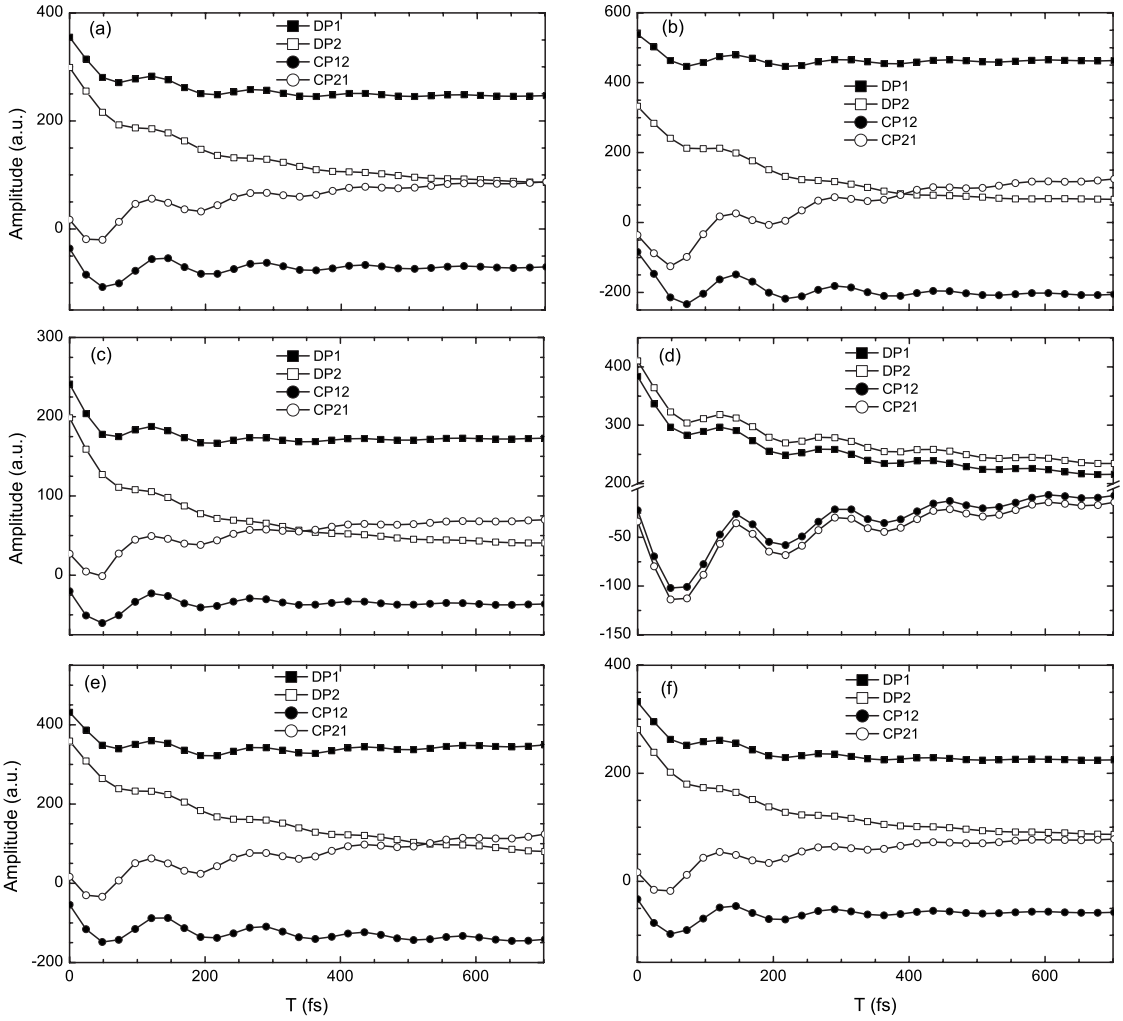

FIG. 6. Oscillations of the of the major peak amplitudes of the 2D electronic spectra in the presence of static disorder calculated using different methods. (a) HEOM, (b) TNL2, (c) TL2, (d) SLE, (e) HTA, and (f) modified HTA.

which corresponds to the $(2n)$th order TNL perturbative QME,[45,50,61] can give improved results in calculating the 2D spectra. Figure 4 shows the fourth and sixth order TNL results at $T=97$ and 218 fs. The 2D spectra from the 6th order TNL QME is essentially the same as those from the HEOM. Further increasing of the reorganization energy to 100 cm^{-1} requires the eighth order TNL QME to get converged results (results not shown). Our result indicates that higher order QMEs may be a reasonable approach in calculating nonlinear optical response functions in molecular aggregates when used carefully.

B. The effect of static disorder

Now the static disorder is added by assuming that the on-site energies are described by a Gaussian distribution with a full width at half maximum of 100 cm^{-1}. The orientation disorder is also considered by assuming that the transition dipoles of the two monomers have the same value, but are perpendicular to each other. Figure 5 shows the 2D electronic spectra calculated using different methods. The static disorder is assumed to be independent for the two sites, and a total number of 1000 averages were used in each calculation.

It can be seen that the TNL2 peaks are again too narrow in the antidiagonal direction, which is in contrast to the absorption spectra case,[45] where the effect of inhomogeneous broadening can disguise the inability of the TNL2 method to calculate the correct line shape for a single sample. As is well known, the diagonal widths of 2D spectral peaks represent the inhomogeneous broadening, whereas the antidiagonal widths are related to homogeneous dynamics.[1–5] This result indicates that the TNL2 approach can seriously underestimate the homogeneous broadening.

The TL2 peaks show too large antidiagonal width due to the missing of solvation dynamics. The detailed balance problem of the SLE spectra is also present in the case of static disorder and leads to roughly equal amplitude for two diagonal peaks DP1 and DP2. As in the case without static disorder, the HTA and modified HTA methods give results very similar to the exact HOEM ones.

Oscillations of diagonal and off-diagonal peak amplitudes are plotted in Fig. 6. The curves show more damped beats comparing with Fig. 3, but the oscillations are still visible at $T=400$ fs. As in the case without disorder, the TNL2 and TL2 results give correct behavior for the evolution of peak amplitudes, although the equilibrated peak am-

plitudes are slightly different from the exact result. The SLE result shows stronger oscillations and gives wrong equilibrated peak amplitudes at long times. The HTA and modified HTA curves agree very well with the exact ones.

IV. CONCLUSION

As mentioned in the introduction section, the HEOM method has developed into an important tool to study the dissipative dynamics and related spectroscopy signal in various kind of systems. In this paper, we have extended its application to calculate the 2D spectra in molecular aggregates using model dimer systems. We have also investigated the applicability of several approximate methods closely related to the HEOM method, and the following were found: (1) the widely used second order QMEs show deficiencies in describing peak shapes and solvation dynamics. Since the reorganization energy in the intermediate regime is typically around 100 cm^{-1}, these drawbacks are likely to be corrected when high order perturbative QME is applied. Of course, the convergence of high order QME also depends on other parameters such as the intermolecular coupling strength and the bath relaxation time scale. (2) The SLE is able to give reasonable peak shapes and describe solvation dynamics. However, it cannot correctly describe the evolution of peak amplitudes due to the lack of detailed balance. The HTA results are much improved by including the imaginary part of the bath correlation function. (3) The modified HTA method so far is the most promising approximate method considered in this paper, giving both good peak shapes and amplitude evolution.

As correctly describing the peak shapes and amplitudes are important in explaining the experimental 2D spectra, our results highlight the need for new theories in modeling exciton dynamics and nonlinear spectra in the intermediate coupling regime. Comparing with other recently developed approximate methods such as the modified Lindblad equation,[65] and the QME based on polaron transformation,[66,67] the advantage of the HEOM method lies in its nonperturbative nature and capability to provide numerical exact results for model systems. Further application of the HEOM method to realistic systems would help to explain the experimental findings in various types of molecular aggregates. It should also be noted that the HEOM presented in this paper are derived for Gaussian bath dynamics, while it is found recently that non-Gaussian dynamics play an important role in the 2D IR spectra of hydrogen bonded liquids.[37,68] Although the SLE/NISE methods[36–38] can easily be applied to investigate the effect of non-Gaussian dynamics, extending the HEOM method to general non-Gaussian bath dynamics is still an on-going challenge.

ACKNOWLEDGMENTS

This work is supported by NNSF of China (Grant Nos. 20733006, 20873157, and 20903101), the Chinese Academy of Sciences (Grant No. KJCX2.YW.H17 and the Hundred Talents Project), and the RGC Hong Kong (Grant Nos. 604508 and 604709).

[1] S. Mukamel, Y. Tanimura, and P. Hamm, eds., *Coherent Multidimensional Optical Spectroscopy*, Special Issue of Acc. Chem. Res. **42**, 1207 (2009).
[2] S. Mukamel and D. Abramavicius, Chem. Rev. (Washington, D.C.) **104**, 2073 (2004).
[3] M. Cho, Chem. Rev. (Washington, D.C.) **108**, 1331 (2008).
[4] D. M. Jonas, Annu. Rev. Phys. Chem. **54**, 425 (2003).
[5] M. Khalil, N. Demirdöven, and A. Tokmakoff, J. Phys. Chem. A **107**, 5258 (2003).
[6] P. Hamm, M. Lim, and R. M. Hochstrasser, J. Phys. Chem. B **102**, 6123 (1998).
[7] J. B. Asbury, T. Steinel, K. Kwak, S. A. Corcelli, C. P. Lawrence, J. L. Skinner, and M. D. Fayer, J. Chem. Phys. **121**, 12431 (2004).
[8] J. D. Hybl, A. A. Ferro, and D. M. Jonas, J. Chem. Phys. **115**, 6606 (2001).
[9] M. Cho, H. M. Vaswani, T. Brixner, J. Stenger, and G. R. Fleming, J. Phys. Chem. B **109**, 10542 (2005).
[10] A. M. Moran, J. B. Maddox, J. W. Hong, J. Kim, R. A. Nome, G. C. Bazan, S. Mukamel, and N. F. Scherer, J. Chem. Phys. **124**, 194904 (2006).
[11] T. Brixner, J. Stenger, H. M. Vaswani, M. Cho, R. E. Blankenship, and G. R. Fleming, Nature (London) **434**, 625 (2005).
[12] G. S. Engel, T. R. Calhoun, E. L. Read, T.-K. Ahn, T. Mancal, Y.-C. Cheng, R. E. Blankenship, and G. R. Fleming, Nature (London) **446**, 782 (2007).
[13] H. Lee, Y.-C. Cheng, and G. R. Fleming, Science **316**, 1462 (2007).
[14] E. Collini and G. D. Scholes, Science **323**, 369 (2009).
[15] E. Collini and G. D. Scholes, J. Phys. Chem. A **113**, 4223 (2009).
[16] T. Kobayashi, *J-Aggregates* (World Scientific, Singapore, 1996).
[17] H. van Amerongen, L. Valkunas, and R. van Grondelle, *Photosythetic Exictons* (World Scientific, Singapore, 2000).
[18] T. Renger, V. May, and O. Kühn, Phys. Rep. **343**, 137 (2001).
[19] I. Stiopkin, T. Brixner, M. Yang, and G. R. Fleming, J. Phys. Chem. B **110**, 20032 (2006).
[20] N. S. Ginsberg, Y.-C. Cheng, and G. R. Fleming, Acc. Chem. Res. **42**, 1352 (2009).
[21] F. Milota, J. Sperling, A. Nemeth, D. Abramavicius, S. Mukamel, and H. F. Kauffmann, J. Chem. Phys. **131**, 054510 (2009).
[22] S. Mukamel, *The Principles of Nonlinear Optical Spectroscopy* (Oxford University, New York, 1995).
[23] W. M. Zhang, T. Meier, V. Chernyak, and S. Mukamel, J. Chem. Phys. **108**, 7763 (1998).
[24] K. Ohta, M. Yang, and G. R. Fleming, J. Chem. Phys. **115**, 7609 (2001).
[25] M. Yang and G. R. Fleming, Chem. Phys. **282**, 163 (2002).
[26] K. Hyeon-Deuk, Y. Tanimura, and M. Cho, J. Chem. Phys. **127**, 075101 (2007).
[27] D. Abramavicius, L. Valkunas, and S. Mukamel, EPL **80**, 17005 (2007).
[28] M. F. Gelin, D. Egorova, and W. Domcke, J. Chem. Phys. **123**, 164112 (2005).
[29] P. Kjellberg and T. Pullerits, J. Chem. Phys. **124**, 024106 (2006).
[30] T. Mančal, A. V. Pisliakov, and G. R. Fleming, J. Chem. Phys. **124**, 234504 (2006).
[31] A. V. Pisliakov, T. Mancal, and G. R. Fleming, J. Chem. Phys. **124**, 234505 (2006).
[32] D. Egorova, M. F. Gelin, and W. Domcke, J. Chem. Phys. **126**, 074314 (2007).
[33] Y.-C. Cheng and G. R. Fleming, J. Phys. Chem. B **112**, 4254 (2008).
[34] R. Kubo, J. Phys. Soc. Jpn. **9**, 935 (1954).
[35] P. W. Anderson, J. Phys. Soc. Jpn. **9**, 316 (1954).
[36] K. Kwac and M. Cho, J. Chem. Phys. **119**, 2256 (2003).
[37] J. R. Schmidt, S. A. Corcelli, and J. L. Skinner, J. Chem. Phys. **123**, 044513 (2005).
[38] T. L. C. Jansen and J. Knoester, Acc. Chem. Res. **42**, 1405 (2009).
[39] T. L. C. Jansen, W. Zhuang, and S. Mukamel, J. Chem. Phys. **121**, 10577 (2004).
[40] T. L. C. Jansen, T. Hayashi, W. Zhuang, and S. Mukamel, J. Chem. Phys. **123**, 114504 (2005).
[41] Q. Shi and E. Geva, J. Chem. Phys. **129**, 124505 (2008).
[42] P. L. McRobbie, G. Hanna, Q. Shi, and E. Geva, Acc. Chem. Res. **42**, 1299 (2009).
[43] G. Hanna and E. Geva, J. Phys. Chem. B **113**, 9278 (2009).
[44] V. M. Kenkre and P. Reineker, *Exciton Dynamics in Molecular Crystals and Aggregates* (Springer, Berlin, 1982).
[45] L. P. Chen, R. H. Zheng, Q. Shi, and Y. J. Yan, J. Chem. Phys. **131**,

094502 (2009).
[46] Y. Tanimura and R. Kubo, J. Phys. Soc. Jpn. **58**, 101 (1989).
[47] Y. Tanimura, Phys. Rev. A **41**, 6676 (1990).
[48] Y. Tanimura, J. Phys. Soc. Jpn. **75**, 082001 (2006).
[49] A. Ishizaki and Y. Tanimura, J. Phys. Soc. Jpn. **74**, 3131 (2005).
[50] R. X. Xu, P. Cui, X. Q. Li, Y. Mo, and Y. J. Yan, J. Chem. Phys. **122**, 041103 (2005).
[51] R. X. Xu and Y. J. Yan, Phys. Rev. E **75**, 031107 (2007).
[52] T. Kato and Y. Tanimura, J. Chem. Phys. **120**, 260 (2004).
[53] A. Ishizaki and Y. Tanimura, J. Chem. Phys. **125**, 084501 (2006).
[54] A. Ishizaki and Y. Tanimura, J. Phys. Chem. A **111**, 9269 (2007).
[55] A. Ishizaki and G. R. Fleming, J. Chem. Phys. **130**, 234110 (2009).
[56] A. Ishizaki and G. R. Fleming, J. Chem. Phys. **130**, 234111 (2009).
[57] A. Ishizaki and G. R. Fleming, Proc. Natl. Acad. Sci. U.S.A. **106**, 17255 (2009).
[58] M. Cho, J. Chem. Phys. **115**, 4424 (2001).
[59] A. Ishizaki and Y. Tanimura, Chem. Phys. **347**, 185 (2008).
[60] Q. Shi, L. P. Chen, G. J. Nan, R. X. Xu, and Y. J. Yan, J. Chem. Phys. **130**, 084105 (2009).
[61] M. Schröder, M. Schreiber, and U. Kleinekathöfer, J. Chem. Phys. **126**, 114102 (2007).
[62] H. P. Breuer and F. Petruccione, *The Theory of Open Quantum Systems* (Oxford University, New York, 2002).
[63] R. X. Xu, B. L. Tian, J. Xu, Q. Shi, and Y. J. Yan, J. Chem. Phys. **131**, 214111 (2009).
[64] Y.-C. Cheng, G. S. Engel, and G. R. Fleming, Chem. Phys. **341**, 285 (2007).
[65] B. Palmieri, D. Abramavicius, and S. Mukamel, J. Chem. Phys. **130**, 204512 (2009).
[66] S. Jang, Y.-C. Cheng, D. R. Reichman, and J. D. Eaves, J. Chem. Phys. **129**, 101104 (2008).
[67] S. Jang, J. Chem. Phys. **131**, 164101 (2009).
[68] T. C. Jansen, D. Cringus, and M. S. Pshenichnikov, J. Phys. Chem. A **113**, 6260 (2009).